Insights into cytoskeletal behavior from computational modeling of dynamic microtubules in a cell-like environment

Ivan V. Gregoretti[1,2], Gennady Margolin[1,3], Mark S. Alber[1,3] and Holly V. Goodson[1,2,*]

[1]Interdisciplinary Center for the Study of Biocomplexity, [2]Department of Chemistry and Biochemistry and [3]Department of Mathematics, University of Notre Dame, Notre Dame, IN 46556 USA

*Author for correspondence (e-mail: hgoodson@nd.edu)

Summary

Microtubule dynamic instability plays a fundamental role in cell biology, enabling microtubules to find and interact with randomly distributed cargo and spatially localized signals. In vitro, microtubules transition between growth and shrinkage symmetrically, consistent with the theoretical understanding of the mechanism of dynamic instability. In vivo, however, microtubules commonly exhibit asymmetric dynamic instability, growing persistently in the cell interior and experiencing catastrophe near the cell edge. What is the origin of this behavior difference? One answer is that the cell edge causes the asymmetry by inducing catastrophe in persistently growing microtubules. However, the origin of the persistent growth itself is unclear. Using a simplified coarse-grained stochastic simulation of a system of dynamic microtubules, we provide evidence that persistent growth is a predictable property of a system of nucleated, dynamic, microtubules containing sufficient tubulin in a confined space – MAP activity is not required. Persistent growth occurs because cell-edge-induced catastrophe increases the concentration of free tubulin at steady-state. Our simulations indicate that other aspects of MT dynamics thought to require temporal or spatial changes in MAP activity are also predictable, perhaps unavoidable, outcomes of the 'systems nature' of the cellular microtubule cytoskeleton. These include the mitotic increase in microtubule dynamics and the observation that defects in nucleation cause changes in the behavior of microtubule plus ends. These predictions are directly relevant to understanding of the microtubule cytoskeleton, but they are also attractive from an evolutionary standpoint because they provide evidence that apparently complex cellular behaviors can originate from simple interactions without a requirement for intricate regulatory machinery.

Supplementary material available online at
http://jcs.biologists.org/cgi/content/full/119/22/4781/DC1

Key words: Microtubule dynamic instability, Stochastic simulation, Emergent properties

Introduction

Microtubules (MTs) are components of the cytoskeleton, the network of proteinaceous fibers that endows the cell with structural integrity, motile properties, and internal organization. MTs play a particularly important role in cell organization: they pull the chromosomes apart at mitosis, act as a 'railroad system' for intracellular transport, and define the localization and structure of internal membrane systems (Kline-Smith and Walczak, 2004; Musch, 2004; Rogers and Gelfand, 2000). Two characteristics of MTs are particularly significant for these functions. First, MT nucleation is regulated, and the limitation of nucleation to an organelle near the nucleus (the centrosome) endows most cell types with a radial organization. Second, and perhaps more importantly, the MT cytoskeleton is dynamic: individual MTs in the same cell (or same test tube) constantly change in length, either growing or shrinking with random transitions between these phases (Desai and Mitchison, 1997).

This counterintuitive behavior is termed dynamic instability and is fundamental to MT function. First, dynamic instability is a mechanism for exploring cellular space, bringing MT

railroads into contact with poorly diffusible cargo, such as chromosomes for subsequent transport (Hill, 1985; Holy and Leibler, 1994; Mitchison and Kirschner, 1984; Wollman et al., 2005). Second, this turnover ensures rapid response of the cytoskeleton to internal and external signals. Selective stabilization of dynamic MTs probably plays a key role in morphogenesis and appears to play a central role in the self-organizing properties of the mitotic spindle (Heald et al., 1996; Kirschner and Mitchison, 1986; Wollman et al., 2005).

Understanding the role of MTs in cell organization requires a detailed understanding of dynamic instability and its regulation. MTs are noncovalent polymers of the protein tubulin. Dynamic instability originates in conformational changes that occur in tubulin subunits after polymerization. Briefly, tubulin subunits (which are obligate dimers of the polypeptides α- and β-tubulin) bind GTP. Upon polymerization, this GTP is hydrolyzed to GDP, but only after a short delay. This delay is thought to result in a 'GTP cap', which predisposes the MT to continued growth. The idea is that if this cap is lost (via hydrolysis or other mechanism), the exposed GDP-tubulin subunits rapidly depolymerize in an

event termed catastrophe (reviewed in Desai and Mitchison, 1997). This elegant explanation has recently been modified to include the possibility that the conformational state of the tubulin subunits in the cap may be more important than the state of the bound nucleotide (Arnal et al., 2000; Chretien et al., 1995; Wang and Nogales, 2005). Dynamic instability occurs in solutions of pure tubulin and GTP, but it can be modulated by a variety of MT-binding proteins (also called microtubule-associated proteins or MAPs), including MAP4, stathmin, and CLIP-170 (Andersen, 2000; Arnal et al., 2004; Desai and Mitchison, 1997).

Although this molecular-level explanation has been extremely useful, many aspects of MT behavior remain poorly understood. In particular, what determines dynamic-instability parameters? One expects them to be a function of fundamental chemical parameters (association constants, dissociation constants and hydrolysis rates) and environmental parameters (the concentration of tubulin, the number of nucleation sites and the presence of spatial constraints), but no complete mathematical description of the relationship between these quantities has been derived. A major reason for this incomplete understanding is that dynamic instability is an emergent phenomenon – a behavior that arises from the independent interaction of many individual components, resulting in system-level properties that are not obviously predictable from the characteristics of the components.

One approach that has proven useful for studying such complex systems is computational modeling, in which the behavior of a system is simulated by allowing components of the system to interact according to defined rules. Insight into the system is obtained by seeing how the system changes when the rules are altered, and comparing these observations to expectation or experiment. Significant efforts have been made to predict and explain MT behavior using both deterministic models (systems of interacting equations) and stochastic simulations (Markov chain/Monte Carlo approaches) (e.g. Bayley et al., 1989; Bolterauer et al., 1999; Dogterom and Leibler, 1993; Flyvbjerg et al., 1996a; Freed, 2002; Gliksman et al., 1993; Govindan and Spillman, Jr, 2004; Hill and Chen, 1984; VanBuren et al., 2002).

These studies have provided insight into numerous aspects of MT behavior, including the origin of dynamic instability, the nature of the stabilizing cap, and the effect of physical boundaries on MT length distributions. However, many of these efforts examine the behavior of single MTs. Those with multiple MTs occur in semi-infinite space and/or have variables, such as tubulin concentration or transition frequencies, defined to be constants. None of these studies examines how the behavior of MTs is influenced by the constraints of a cell-like environment, in which multiple MTs (but not an infinite number) compete for a limited pool of tubulin subunits and microtubule growth is spatially confined.

To begin to address these issues, we have performed a series of Monte-Carlo simulations of a system of dynamic MT in such a cell-like environment. In these simulations, MTs (nucleated by a defined number of seeds) compete with each other for free GTP tubulin subunits in a 'cell' of defined size and shape. MTs can be followed visually or statistically at the level of an individual or the population. Dynamic instability parameters (transition frequencies, growth rates, and shrinkage rates) are not set by the user but instead evolve from the

interactions of the different parts of the system as the simulation proceeds. A recent article by Janulevicius et al. (Janulevicius et al., 2006) describes a model that has similarities to the one we used here, but which was used to address different questions.
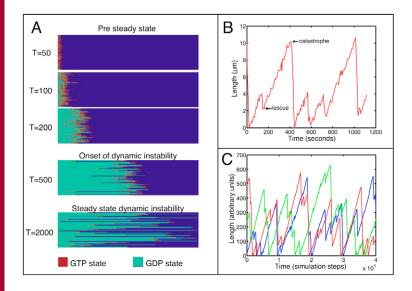
Using our model, we find that several cellular phenomena that were thought to require complex regulatory machinery are instead predictable outcomes of interactions between a system of dynamic MTs and its physical environment. More specifically, we find that the surprisingly persistent growth of MTs observed in vivo is a predictable property of a nucleated system of dynamic MTs containing sufficient tubulin and polymerizing in a constrained space. This perturbation of MT dynamics is an outcome of the increase in the steady-state concentration of free tubulin, resulting from interactions of MTs with the cell boundary. Similarly, changes in nucleation activity are expected to have major effects on MT length and transition frequencies, dictating changes such as those seen at the interphase-mitosis transition (Piehl et al., 2004; Rusan et al., 2001). These observations do not exclude MAP involvement (obviously, MAPs play central roles in these processes), but they imply that MAPs modulate these behaviors instead of creating them. These studies indicate that the classic concept of critical concentration requires revision when applied to cellular systems, and they provide a foundation for quantitative understanding of MT dynamics in vitro and in vivo.

Results and Discussion
Recapitulation of dynamic instability by our Monte Carlo model

Using the rules outlined in the Materials and Methods, we have built a simplified coarse-grained stochastic simulation of MT dynamics that incorporates the major elements of the MT polymerization process in vivo, including spatially constrained nucleation, competition between MTs for tubulin subunits, and the imposition of physical limitations to MT polymerization by the cell edge. Adjustable parameters are the total tubulin concentration, cell size, rate of GTP hydrolysis, and association and dissociation rate constants for GTP and GDP tubulin. MT dynamic instability parameters (rate of growth, rate of depolymerization, catastrophe frequency, and rescue frequency) are not set by the modeler but instead change with time and conditions, emerging from the dynamic interactions of the system. This model recapitulates the obvious qualitative features of dynamic instability (Fig. 1, Movie 1 in supplementary material). When appropriate adjustable parameters are chosen (see Materials and Methods), it can approximate the quantitative features, including growth rate and transition frequencies (Table 1). Unless otherwise indicated, all data presented in this manuscript are obtained from simulations run under a set of reference parameters chosen to approximate the behavior of tubulin in vivo in interphase (Rusan et al., 2001), and are from steady-state (see Materials and Methods for details).

This model is similar to the stochastic simulations used by Hill and Chen (Hill and Chen, 1984), but there are two key differences. First, in our model, a system of dynamic MTs is simulated instead of a single MT, and the concentration of soluble tubulin ($[Tu]_{soluble}$) in this system changes as MTs grow and compete for subunits (in most previous simulations,

Fig. 1. Recapitulating dynamic instability. (A) Snapshots of the simulation at different time steps (T). The MTs grow from seeds at left towards the 'cell' edge (right). The colors describe the state (red, GTP ; green, GDP) of each subunit. At early times, when free tubulin is near the initial value, MTs grow persistently. As the polymer fraction increases and the concentration of free tubulin drops, catastrophe becomes more frequent. Eventually the steady-state is reached, and the system behavior exhibits behavior very similar to experimentally observed dynamic instability (see Movie 1, supplementary material). (B,C) Comparison between life history plots obtained experimentally in vitro (B) and with our model (C). Experimental data were adapted from Fygenson et al. (Fygenson et al., 1994). C shows three adjacent steady-state MTs from the simulation shown in (A). In this simulation, parameters were chosen arbitrarily; all other simulations reported in this manuscript are correlated to physiological concentrations and dimensions as described in Materials and Methods.

including those of Hill, $[Tu]_{soluble}$ is a set parameter). Second, we have imposed MT-length limits (analogous to the limitations imposed by the cell boundary). The sum of these characteristics suggests that this model is useful for investigating the constraints on MT dynamics imposed by cell-like systems.

Persistent growth of MTs in vivo and in silico

Perturbation of the simulation by changing the concentration of total tubulin ($[Tu]_{total}$), leaving all other parameters unaltered, reveals an important relationship between tubulin concentration and MT behavior. At low $[Tu]_{total}$, MTs in the simulation mimic MTs observed in vitro at steady-state: catastrophe is frequent, rescue is relatively rare and MT lengths decay exponentially (short MTs significantly outnumber long MTs) (Fig. 2A,E, Table 1, Movie 2 in supplementary material). However, at relatively high $[Tu]_{total}$, dramatically different behavior is observed: MTs begin to grow persistently, meaning that many MTs reach the cell edge without ever undergoing catastrophe (Fig. 2B and Table 1, Movie 3 in supplementary material). Most catastrophes occur near the cell edge and rescue becomes more frequent, resulting in an accumulation of MT ends near the cell edge (Fig. 2F). This behavior mimics that observed in vivo (Komarova et al., 2002b).

What is the origin of this change from an in-vitro-like behavior to an in-vivo-like behavior? The observation that catastrophe frequency displays position dependence in vivo has been addressed previously: Komarova et al. and Maly et al. have suggested that the cell edge induces catastrophe in persistently growing MTs, causing the catastrophe asymmetry and resulting in the MT length distribution observed in vivo (Komarova et al., 2002b; Maly, 2002). Induction of catastrophe by physical boundaries has been observed experimentally (Janson et al., 2003). We have incorporated these ideas into our model by stipulating that the cell edge prevents the addition of new tubulin subunits, resulting in loss of the GTP cap, which then leads to catastrophe.

However, although the 'edge-induced depolymerization' explanation is attractive, it is not complete. It explains the catastrophe asymmetry, but fails to address the key issue of the cause of the persistent growth. Komarova and colleagues proposed that MAP activities are involved, and provided evidence that the MT plus end tracking protein CLIP-170 plays a role in persistent growth (Komarova et al., 2002a). However, the only difference between the simulations in Fig. 2A,B (one exhibiting persistent growth and one not) is the amount of total tubulin in the system.

Consideration of the behavior of our computational model

Table 1. Dynamic instability parameters derived from experiments and simulations

	In vivo[‡]		In silico			
	Interphase	Mitosis	Low $[Tu]_{total}$ 1× no. of MTs	High $[Tu]_{total}$ 1× no. of MTs (interphase-like)	High $[Tu]_{total}$ 4× no. of MTs (mitosis-like)	High $[Tu]_{total}$ 0.25× no. of MTs
Catastrophe frequency (seconds^{-1})	0.026±0.024	0.058±0.045	0.051±0.003	0.033±0.003	0.043±0.003	–
Rescue frequency (seconds^{-1})	0.175±0.104	0.045±0.111	0.070±0.007	0.096±0.006	0.086±0.007	–
Growth rate (μm/second)	0.191±0.123	0.212±0.094	0.095±0.003	0.167±0.004	0.122±0.003	–
Shortening rate (μm/second)	–0.218±0.140	–0.236±0.131	–0.18±0.01	–0.34±0.02	–0.28±0.02	–
Mean MT length (cell radius fraction)	~85%[†]	Shorter than in interphase	0.09±0.01	0.76±0.03	0.23±0.01	0.95±0.03
Initial [Tu] (μM)	–	–	5.0±0.0	14.0±0.0	14.0±0.0	14.0±0.0
Steady-state [Tu] (μM)	–	–	4.10±0.06	6.4±0.1	4.7±0.2	11.64±0.07

The values of the simulations are the mean and standard deviation of 50 repetitions. [‡]In vivo data are from Rusan et al. (Rusan et al., 2001), except [†], which is from Komarova et al. (Komarova et al., 2002b). No numbers are given for the first four cells of the last column because microtubules in these simulations were too close to the boundary to allow accurate measurements. Note that though the precise values of the experiments and simulations do not match (and are not meant to), the trends are similar.
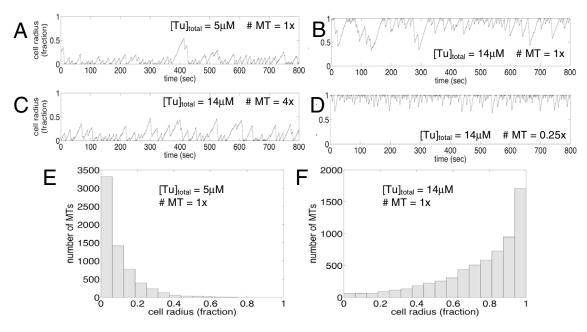
Fig. 2. Relationship between the concentration of total tubulin ($[Tu]_{total}$), the number of MTs and the behavior of MTs in a spatially constrained environment. (A-D) Life history plots of representative MTs in simulations run under the indicated conditions. (E,F) Distribution of MT lengths taken from a series of simulations conducted under the indicated conditions.

leads to an alternative hypothesis for the origin of the persistent growth: (1) the cell boundary induces catastrophe prematurely (Komarova et al., 2002b; Maly, 2002); (2) this catastrophe induction causes $[Tu]_{soluble}$ at steady-state to be higher than it would be in the absence of the barrier; (3) this higher availability of $[Tu]_{soluble}$ is what allows the MTs to grow persistently, experiencing few catastrophes and undergoing more frequent rescues. This hypothesis predicts that a physical boundary can cause the $[Tu]_{soluble}$ steady-state to rise above its natural steady-state level, and this increase in $[Tu]_{soluble}$ can be sufficient to cause persistent MT growth.

Relationship between total tubulin and soluble tubulin: expected behavior according to the classic model

As a first test of this hypothesis, we investigated the relationship between $[Tu]_{total}$ and $[Tu]_{soluble}$ at steady-state. Before examining our system, we wanted to first understand what was expected from the existing literature. The classic understanding of monomer/polymer partitioning as defined by Oosawa and colleagues, and refined by Johnson and Borisy is shown in Fig. 3A (Johnson and Borisy, 1977; Oosawa and Asakura, 1975; Oosawa and Kasai, 1962), see also Howard for a more recent discussion (Howard, 2001). Examination of this figure shows that tubulin put into a system is expected to remain unpolymerized until the concentration of unpolymerized tubulin reaches a critical concentration, after which point all additional tubulin is incorporated into polymer. Under this model, $[Tu]_{soluble}$ remains at the critical concentration no matter how much additional tubulin is added (assuming that all of it is active).

Deviation from this expected behavior

This Oosawa model has been the dominant framework for understanding bulk MT polymerization. Our model reproduces this expected behavior when MT length is unconstrained

(compare red solid curves in Fig. 3A,B)[1]. However, when MT length is physically constrained – as it would be in a cell – the concentration of soluble tubulin deviates significantly from the behavior according to the classic model (Fig. 3B, dashed curve): there is no clearly observed critical concentration and, instead of plateauing after the initial rise, $[Tu]_{soluble}$ continues to rise with $[Tu]_{total}$, at first slowly and then more quickly. Because the two curves of Fig. 3B are produced under conditions that are identical except for the presence or absence of catastrophe induction by the cell edge, these observations suggest that the 'edge effect' predicted above can cause $[Tu]_{soluble}$ to rise above that expected from standard considerations of critical concentration[2]. Moreover, the effect increases as more tubulin is added to the system.

Effect of small changes in the $[Tu]_{soluble}$ on MT behavior

We next examined the effect of such changes in $[Tu]_{soluble}$ on MT behavior. The differences seen between the solid and dashed lines of the curves in Fig. 3B are relatively small: when $[Tu]_{total}$ rises from 5 μM to 14 μM, $[Tu]_{soluble}$ rises only from ~4 to ~6 μM, respectively. Although this increase may seem

---

[1]The sharper transition to the plateau of the curve in panel A (compared with the curve in panel B) results from the fact that the model used to yield curve A incorporates a very unfavorable nucleation step, which normally exists when tubulin polymerizes in vitro. Our model, which is meant to simulate microtubule polymerization from stable nucleation sites in vivo, produces a similarly sharp transition if the difficulty in initial growth from the stable seeds is increased (supplementary material Fig. S1).

[2]In 1987, Mitchison and Kirschner performed a theoretical analysis suggesting that $[Tu]_{soluble}$ increases with $[Tu]_{total}$ in mass- and number-limited systems of dynamic microtubules, such as those in a cell, even in the absence of spatial constraint (Mitchison and Kirschner, 1987). Some of their conclusions are similar to those discussed here. However, their conclusions depend on the assumption that rescue does not occur. Because rescue is common in cellular systems, and because our simulations behave according to their predictions only when both rescue and spatial constraint are 'turned off' (supplementary material Fig. S1), we believe that the conclusions of their analysis were prescient but the equations leading to these conclusions are of limited use.
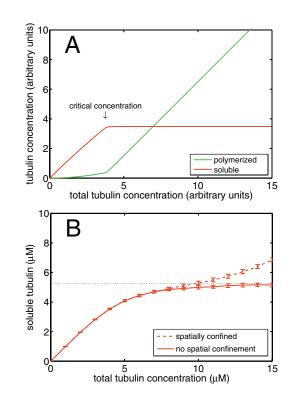
Fig. 3. Relationships between total tubulin and soluble tubulin ([Tu]$_{soluble}$) at steady-state. (A) Classically expected behavior. Note that little polymer is seen until the critical concentration (C$_c$) is achieved. At total tubulin concentrations above C$_c$, all additional tubulin is incorporated into polymer, and the concentration of unpolymerized tubulin remains at C$_c$. See Materials and Methods for the equations used to plot these curves. (B) Relationship observed in our simulations. Solid red line: system without spatial confinement. Dashed red line: system with spatial confinement. The dotted grey line gives C$_c$ (i.e. [Tu]$_{soluble}$) that is asymptotically approached as [Tu]$_{total}$ increases. Notice that, in confined systems there is no easily observed C$_c$. Instead, the concentration of free tubulin continues to rise as total tubulin rises, at first slowly, and then more steeply. The curves in B are not fits to an equation but are provided to guide the eye as it follows the progression of the data.

insignificant, Fig. 4 shows that it is predicted to have a major effect on the behavior of the simulated MTs: Changing [Tu]$_{soluble}$ from 4.1 µM to 6.4 µM shifts the behavior of the simulated MTs from classic dynamic instability to apparently persistent growth (Fig. 4A). Note that, to test the dependence of MT behavior on [Tu]$_{soluble}$ as in Fig. 4A, it is necessary to hold [Tu]$_{soluble}$ constant (i.e. we altered the simulation so that in these trials the MTs do not compete for tubulin. In addition, there is no spatial constraint).

To better understand this transition to persistent growth, we examined the relationship between [Tu]$_{soluble}$ and average MT length in more detail. When [Tu]$_{soluble}$ is held constant at low to moderate levels, the length of MTs at steady-state increases as soluble tubulin increases, but it is finite across this concentration range (Fig. 4B). However, as [Tu]$_{soluble}$ increases more, there is a narrow range in which the average steady-state length rises steeply, appearing to approach infinity at some threshold (between 5 and 6 µM soluble tubulin under these conditions) (Fig. 4B). This threshold is

the transition to persistent growth – as can be seen in a plot of net MT growth rate as a function of [Tu]$_{soluble}$ (Fig. 4C). When this threshold is passed, MTs still experience catastrophes but the balance between catastrophe and rescue is such that, the amount of polymer in such a system increases constantly with time (Fig. 4A,C). On the basis of this analysis, small increases in the steady-state concentration of soluble tubulin (like those caused by interaction of MTs with the cell edge) should induce persistent growth if the initial [Tu]$_{soluble}$ is close enough to the persistent growth threshold. Note that the transition to persistent growth occurs at a concentration empirically similar to the critical concentration observed in the absence of spatial constraint (compare the dotted line in Fig. 3B with the x-axis intercept of the dashed line in Fig. 4C), but we have not yet developed a formal demonstration of this relationship.
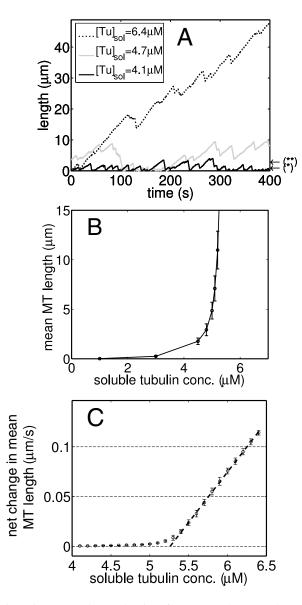
These observations are consistent with previous analyses indicating that average MT length should increase with [Tu]$_{soluble}$, and that MTs should show a transition from 'bounded' to 'unbounded' growth when [Tu]$_{soluble}$ passes a threshold (Dogterom and Leibler, 1993; Verde et al., 1992). In a physiological system, the total mass of tubulin is constant, and competition between MTs for this tubulin would be expected to keep [Tu]$_{soluble}$ below the transition to persistent growth. However, if a physical boundary limits polymerization and the edge effect (Fig. 3B) causes [Tu]$_{soluble}$ to rise above the threshold, persistent growth should occur.

One conclusion of this work is that the classic concept of critical concentration must be used carefully in cellular systems – [Tu]$_{soluble}$ at steady-state is not simply equal to the critical concentration. Instead, the steady-state [Tu]$_{soluble}$ is a dynamic parameter that depends on a host of variables including the number of nucleation sites, the total amount of tubulin and the cell size. Transition frequencies and MT length distribution are coupled to these same variables through [Tu]$_{soluble}$. As originally suggested by Mitchison and Kirschner (Mitchison and Kirschner, 1987), the increase of [Tu]$_{soluble}$ with [Tu]$_{total}$ is probably a major part of the mechanism, allowing total tubulin levels to be tightly regulated in vivo.

On the basis of these simulations and the reasoning above, we propose that the persistent growth of MTs observed in vivo is an expected outcome of placing a sufficient amount of tubulin in a spatially confined system under conditions where nucleation is limited. This reasoning does not exclude the involvement of MT-binding proteins in persistent growth in vivo, but argues that they tune the behavior instead of generating it. Although physiological systems differ from our simulations (and from each other) in their quantitative details, this analysis suggests that persistent growth in the presence of an appropriate spatial constraint is an intrinsic property of any system of MTs or, indeed, of any nucleated two-state polymer system.

Effect of MT nucleation on MT dynamics

A key aspect of MT growth, both in vivo and in our model, is that it normally occurs from stable nuclei or 'seeds'. We were interested to see whether our simulations could provide insight into two experimental observations related to nucleation: (1) the changes in MT length and dynamics seen together with increases in nucleation during mitosis; (2) the ability of

Fig. 4. Dependence of MT behavior on the concentration of soluble tubulin ([Tu]$_{sol}$) available at steady-state. (A) Life-history plots of individual MTs at different values of [Tu]$_{soluble}$. * and **, average length of MTs at steady-state in 4.1 μM and 4.7 μM free tubulin, respectively. At 6.4 μM free tubulin, there is no steady-state length – the mass of polymer increases with time (MT growth is 'unbound'; see also supplementary material Fig. S1); (B) relationship between [Tu]$_{soluble}$ and the mean MT length at steady-state. (C) Relationship between persistent growth and [Tu]$_{soluble}$. The data plotted on the *y*-axis give average rates of increase in polymer length as a function of [Tu]$_{soluble}$. The concentration of free tubulin required for the transition to persistent growth is indicated by the *x*-axis intercept of the dashed line. In B and C, error bars give the standard deviation of values observed from 50 different simulations at the indicated [Tu]$_{soluble}$. Notice that, in all three panels, the MTs do not compete with each other for free tubulin (because free tubulin is held constant at the indicated value), and the cell size is made so large so that no MTs interact with the edge during the course of the simulation. This is similar to an experimental situation in vitro in which the pool of free tubulin is not depleted during the time course of the experiment.

reduction in [Tu]$_{soluble}$ results from the decreased likelihood of edge-induced catastrophe: when a given mass of tubulin is split between a greater number of microtubules, the MTs get shorter, eventually reaching a natural length that is too short to interact significantly with the cell boundary (compare Fig. 2B with 2C). These considerations suggest that, the increase in MT dynamics observed in vivo during mitosis is an obligatory consequence of the observed increase in MT nucleation. Note that, this assumes that nucleation is controlled directly. An alternative hypothesis is that MAPs could increase the frequency of catastrophes, causing [Tu]$_{soluble}$ to rise. Given that MT growth from centrosomes is reported to increase with [Tu]$_{soluble}$, an increase in [Tu]$_{soluble}$ could cause the observed increase in the number of MTs. The main point of this analysis is to stress the obligatory connection between [Tu]$_{total}$, [Tu]$_{soluble}$, microtubule number and transition frequencies.

Implications for the interpretation of nucleation mutants
Similarly, reducing the number of seeds can be expected to have profound effects on MT length and dynamics (Table 1, Fig. 2, supplementary material Fig. S2). Mutations in γ-tubulin-complex proteins, which cause defects in MT nucleation, also cause abnormalities in MT dynamics, including inappropriately continuous growth, abnormally long MTs, increased growth rate, and catastrophe defects (Zimmerman and Chang, 2005). A number of explanations have been proposed for these effects, including inappropriate regulation of MT-binding proteins, such as Tip1p. Our analysis suggests that, these effects are expected outcomes of the increase in the steady-state concentration of soluble tubulin that is predicted to result from reduction in the number of MTs (Fig. 2D, compare with 2B; Table 1; supplementary material Fig. S2).

Implications for the study of MAPs
Although we did not directly study MAPs in these simulations, our analysis has implications for the understanding of MAP function. Experimental characterization of MAPs has often produced conflicting results (e.g. Cassimeris, 2002; McNally, 2003). We propose that some of the discrepancies stem from

mutations in *S. pombe* nucleation factors to alter MT length and dynamics. In both cases, the effects on MT length and dynamics have been proposed to result from the direct action of MAPs.

Implications for the transition to mitosis
When cells transition into mitosis, the MT cytoskeleton changes from a relatively stable interphase array that has long, persistently growing MTs into an early mitotic array that has shorter, more numerous MTs that are also more dynamic (Piehl et al., 2004; Rusan et al., 2001). Using our computational model, we investigated the relationship between these characteristics. We found that, simply increasing the number of MT seeds in an interphase-like simulation causes the system to adopt mitosis-like dynamic instability characteristics: MTs become significantly shorter and more dynamic, undergoing more spontaneous (not-edge-induced) catastrophes and fewer rescues (Fig. 2C, compare with 2B, Table 1).

These changes in length and dynamics result from the reduction in [Tu]$_{soluble}$ that occurs as the number of nucleation sites is increased (supplementary material Fig. S2). This

failure to take into account the fact that a solution of dynamic MTs in vitro is an evolving system. For example, a protein that suppresses catastrophe without altering other parameters under pre-steady-state conditions (when $[Tu]_{soluble}$ is near the initial concentration) could have little or no effect on catastrophe at steady-state because the protein would reduce $[Tu]_{soluble}$ at steady-state, and catastrophe frequency increases as $[Tu]_{soluble}$ decreases. Indeed, such a protein could have the paradoxical effect of slowing MT growth under steady-state conditions. These issues highlight the systems nature of the MT cytoskeleton and suggest that comprehensive understanding of MAP function is likely to require integration between experimental and computational approaches.

Concluding remarks

We have provided evidence that several aspects of MT dynamics that are often thought to be imposed by MAP activity (or changes in MAP activity) are instead simple, perhaps unavoidable, outcomes of the systems nature of the cellular MT cytoskeleton. More specifically, we find that the surprising persistent growth of MTs observed in vivo is a predictable property of a nucleated system of dynamic MTs polymerizing in a constrained space. Moreover, our simulations indicate that the increase in MT dynamics seen in mitosis is an expected outcome of the mitotic increase in nucleation activity. Similarly, our work provides an explanation for the observation that defects in nucleation cause abnormally stable MT plus ends, without invoking action of nucleation factors at MT plus ends. Our simulations indicate that these effects are mediated by changes in the concentration of free tubulin in the system at steady-state.

We do not mean to imply that regulatory proteins are not involved in behaviors such as persistent growth and the transition to mitosis – it is clear that MAPs play central roles in these processes. However, we suggest that, instead of causing these behaviors, this regulatory machinery tunes them, for example by shifting the amount of free tubulin available or the concentration of free tubulin at which persistent growth occurs.

A pressing question in the history of eukaryotic life is how complex cellular processes arise. Our work indicates that certain behaviors are intrinsic to a system of dynamic microtubules in a confined space. It seems plausible that cells with a rudimentary microtubule array could then, over time, develop machinery to modulate these intrinsic behaviors. This hypothesis is attractive from an evolutionary perspective because it provides evidence that complex cellular behaviors can have simple origins.

Materials and Methods

Essential features of the simulation

MTs are modeled as simple linear polymers of tubulin subunits, with addition and loss of subunits from the tip occurring according to probabilities defined by the following rules: (1) Tubulin subunits have two states that are assumed to be GTP- and GDP-bound, but these states could represent other conformations. (2) Subunits polymerize (add to the end of a MT or seed) in the GTP-bound state, then undergo GTP hydrolysis after polymerization. (3) Hydrolysis of a given subunit occurs according to a set probability that is independent of the nucleotide state of the surrounding subunits, i.e. hydrolysis is a stochastic first order process, producing a shifting 'cap' of GTP subunits of variable length. (4) The probability of subunit-addition or -loss on a MT depends on the nucleotide state of the tubulin subunit exposed at the tip. (5) Subunit addition at the tip depends on the concentration of $[Tu]_{soluble}$, whereas subunit loss is independent of $[Tu]_{soluble}$. (6) The total number of tubulin subunits in the system is fixed (unless otherwise indicated), resulting in competition between microtubules for tubulin subunits and evolution of dynamic-instability parameters as the simulation proceeds. (7) The maximum length of

microtubules is limited by a boundary (analogous to the cell edge). This is summarized in the following mathematical terms:

$$P_{hydrolysis} = K_{hydrolysis} \Delta t,$$

$$P_{growth} = \begin{cases} K_{growth}^{GTP} [Tu]_{soluble} \Delta t & \text{if the tip is in GTP state,} \\ K_{growth}^{GDP} [Tu]_{soluble} \Delta t & \text{if the tip is in GDP state} \end{cases}$$

and

$$P_{shortening} = \begin{cases} 0 & \text{if the tip is in GTP state,} \\ K_{shortening}^{GDP} \Delta t & \text{if the tip is in GDP state.} \end{cases}$$

(1)

Note that, because the model is stochastic, probability transition constants (K) are used in place of kinetic rate constants (k).

Parameter determination

The number of MT-nucleation sites, the size of the pool of tubulin subunits and the size of the cell are set by the user. Unless otherwise indicated, the simulations were run at $[Tu]_{total}$=14 μM, 128 stable seeds (nucleation sites) and cell radius =10 μm. These values were arbitrarily chosen within the range that is biologically plausible (while mammalian cells have many MTs, yeast cells have few) and computationally rapid. Probability transition constants can be varied, but for the purpose of these simulations they were set to constant values chosen to qualitatively approximate the behavior observed in mammalian cells during interphase (Rusan et al., 2001). Specific constants used were K_{growth}^{GTP}=2 μM^{-1} seconds^{-1}, K_{growth}^{GDP}=0.1 μM^{-1} second^{-1}, $K_{shortening}^{GDP}$=48 seconds^{-1}, $K_{shortening}^{GTP}$=0 seconds^{-1}, $K_{hydrolysis}$=0.1 seconds^{-1}. Note that, because the microtubules are modeled as simple linear polymers with subunits that are larger than tubulin (20 nm vs 8 nm), these rate constants do not correspond to experimentally determined values. We emphasize that, the purpose of these simulations is to explore the relationships common to microtubule systems in general, not to quantitatively replicate specific experimental observations. All other parameters of the system (growth rates, depolymerization rates, transition frequencies, concentrations of polymeric and soluble tubulin) are emergent properties. Varying the user-defined constants over a large range changed the specific values of the emergent parameters but did not alter the basic relationships discussed in the text (data not shown).

Other aspects of the model

Induction of catastrophe by the simulation boundary (cell edge) is an indirect result of inhibition of new subunit addition at the boundary, which leads to loss of the GTP cap and eventual depolymerization. In some cases (indicated in the text), simulations were run without spatial constraint, allowing unlimited MT length. Some simulations (as indicated) were also run without constraints on the mass of total tubulin (i.e. constant soluble tubulin). Both tubulin diffusion and regeneration of GTP-tubulin from detached GDP-tubulin were assumed to be fast and, therefore, modeled as instantaneous (Brylawski and Caplow, 1983; Odde, 1997). Therefore, although we present the shape of the cell as rectangular in Fig. 1 and as radial in the movies (see supplementary material, Movies 1-3), the actual cell geometry is undefined. Investigations into the effects of finite diffusion rates or alternative geometries are important avenues for future study. We refer to recent work by Janulevicius et al. for analysis of the effects of limited compartment volume, such as those that might be found in cell processes, on microtubule dynamics (Janulevicius et al., 2006).

Computation and analysis of the simulations

The algorithm was coded in C language and run on PCs using Linux operating systems. The output was analyzed and visualized with Matlab 7.0 SP2 (MathWorks, Natick, MA); movies were made from Matlab output with QuickTime Pro (Apple Computer, Inc., Cupertino, CA). Calculation of transition-frequencies and -rates was performed with a Matlab script that filtered out the noise, and detected persistent growth and shortening phases. Phase transitions occurring within 1% of cell radius from MT seeds or cell edge were excluded from the calculations. Time conversion is: first simulation step equals 0.02 seconds. Source code for all programs is available upon request. Error bars depicted in figures represent the ± standard deviation of 50 repetitions of each simulation.

Classical relationship between $[Tu]_{total}$ and $[Tu]_{soluble}$

The prediction depicted in Fig. 3A was plotted as described by Johnson and Borisy (Johnson and Borisy, 1975). Briefly, the relationship between C_o ($[Tu]_{total}$) and C_1 ($[Tu]_{soluble}$) is expected to satisfy

$$C_o = \sum_{i=1}^{s-1} i K'^{(i-1)} C_1^i + \sum_{i=s}^{\infty} i K'^{(s-1)} K^{-s} (K C_1)^i .$$

(2)

For Fig. 3A, we used a MT nucleus size (s) of 5, in agreement with previous analysis (Johnson and Borisy, 1975) and chose K=2.86×10^{-1} and K'=1.43×10^{-2} to produce an appropriate shape and plateau position. K and K' have units of inverse concentration.

Limitations of the analysis

This model is an approximation chosen to be general (i.e. not dependent on unknown details of the polymerization process) – consistent with MT behavior observed microscopically – and computationally fast, while still incorporating key aspects of tubulin biochemistry. Necessarily, the model has simplifications, the most obvious of which is that MTs were modeled as simple linear polymers instead of tubes composed of protofilaments. Incorporation of structural detail is an important goal for future work, but we do not expect this simplification to alter our basic conclusions because the rules governing the simulation are largely independent of this structural detail (i.e. the rate of growth is expected to be a linear function of subunit concentration (Flyvbjerg et al., 1996b), regardless of the size of the subunits or the number of protofilaments). A second simplification is that, our simulation assumes that tubulin has two states, with a stochastic transformation between them. It is important to notice that the identity of the two states (GTP and GDP, GDP-P_i and GDP, or open sheet and closed tube) is irrelevant – what is important is that there are two states with different characteristics. There may in fact be several conformational states at the end of the MTs but we assume that one of the transitions is rate-limiting, and it is this rate-limiting transition that we are simulating. We chose stochastic transitions instead of the commonly assumed vectorial hydrolysis because previous modeling efforts have indicated that vectorially catalyzed transitions do not fit the data well (Flyvbjerg et al., 1996a). Given the similarity of the simulation to the behavior of MT systems observed experimentally (Table 1, Figs 1, 2), we believe that this model is an informative approximation.

References

Andersen, S. S. (2000). Spindle assembly and the art of regulating microtubule dynamics by MAPs and Stathmin/Op18. *Trends Cell Biol.* **10**, 261-267.

Arnal, I., Karsenti, E. and Hyman, A. A. (2000). Structural transitions at microtubule ends correlate with their dynamic properties in Xenopus egg extracts. *J. Cell Biol.* **149**, 767-774.

Arnal, I., Heichette, C., Diamantopoulos, G. S. and Chretien, D. (2004). CLIP-170/tubulin-curved oligomers coassemble at microtubule ends and promote rescues. *Curr. Biol.* **14**, 2086-2095.

Bayley, P., Schilstra, M. and Martin, S. (1989). A lateral cap model of microtubule dynamic instability. *FEBS Lett.* **259**, 181-184.

Bolterauer, H., Limbach, H.-J. and Tuszynski, J. A. (1999). Models of assembly and disassembly of individual microtubules: stochastic and averaged equations. *J. Biol. Phys.* **25**, 1-22.

Brylawski, B. P. and Caplow, M. (1983). Rate for nucleotide release from tubulin. *J. Biol. Chem.* **258**, 760-763.

Cassimeris, L. (2002). The oncoprotein 18/stathmin family of microtubule destabilizers. *Curr. Opin. Cell Biol.* **14**, 18-24.

Chretien, D., Fuller, S. D. and Karsenti, E. (1995). Structure of growing microtubule ends: two-dimensional sheets close into tubes at variable rates. *J. Cell Biol.* **129**, 1311-1328.

Desai, A. and Mitchison, T. J. (1997). Microtubule polymerization dynamics. *Annu. Rev. Cell Dev. Biol.* **13**, 83-117.

Dogterom, M. and Leibler, S. (1993). Physical aspects of the growth and regulation of microtubule structures. *Phys. Rev. Lett.* **70**, 1347-1350.

Flyvbjerg, H., Holy, T. E. and Leibler, S. (1996a). Microtubule dynamics: caps, catastrophes, and coupled hydrolysis. *Phys. Rev. E Stat. Phys. Plasmas Fluids Relat. Interdiscip. Topics* **54**, 5538-5560.

Flyvbjerg H, Jobs E, Leibler S. (1996b). Kinetics of self-assembling microtubules: an "inverse problem" in biochemistry. *Proc. Natl. Acad. Sci. USA* **93**, 5975-5979.

Freed, K. F. (2002). Analytical solution for steady-state populations in the self-assembly of microtubules from nucleating sites. *Phys. Rev. E Stat. Nonlin. Soft Matter Phys.* **66**, 061916.

Fygenson, D. K., Braun, E. and Libchaber, A. (1994). Phase diagram of microtubules. *Phys. Rev. E Stat. Phys. Plasmas Fluids Relat. Interdiscip. Topics* **50**, 1579-1588.

Gliksman, N. R., Skibbens, R. V. and Salmon, E. D. (1993). How the transition frequencies of microtubule dynamic instability (nucleation, catastrophe, and rescue) regulate microtubule dynamics in interphase and mitosis: analysis using a Monte Carlo computer simulation. *Mol. Biol. Cell* **4**, 1035-1050.

Govindan, B. S. and Spillman, W. B., Jr (2004). Steady states of a microtubule assembly in a confined geometry. *Phys. Rev. E Stat. Nonlin. Soft Matter Phys.* **70**, 032901.

Heald, R., Tournebize, R., Blank, T., Sandaltzopoulos, R., Becker, P., Hyman, A. and Karsenti, E. (1996). Self-organization of microtubules into bipolar spindles around artificial chromosomes in Xenopus egg extracts. *Nature* **382**, 420-425.

Hill, T. L. (1985). Theoretical problems related to the attachment of microtubules to kinetochores. *Proc. Natl. Acad. Sci. USA* **82**, 4404-4408.

Hill, T. L. and Chen, Y. (1984). Phase changes at the end of a microtubule with a GTP cap. *Proc. Natl. Acad. Sci. USA* **81**, 5772-5776.

Holy, T. E. and Leibler, S. (1994). Dynamic instability of microtubules as an efficient way to search in space. *Proc. Natl. Acad. Sci. USA* **91**, 5682-5685.

Howard, J. (2001). *Mechanics of Motor Proteins and the Cytoskeleton*. Sunderland, MA: Sinauer.

Janson, M. E., de Dood, M. E. and Dogterom, M. (2003). Dynamic instability of microtubules is regulated by force. *J. Cell Biol.* **161**, 1029-1034.

Janulevicius, A., van Pelt, J. and van Ooyen, A. (2006). Compartment volume influences microtubule dynamic instability: a model study. *Biophys. J.* **90**, 788-798.

Johnson, K. A. and Borisy, G. G. (1975). The equilibrium assembly of microtubules in vitro. *Soc. Gen. Physiol. Ser.* **30**, 119-141.

Johnson, K. A. and Borisy, G. G. (1977). Kinetic analysis of microtubule self-assembly in vitro. *J. Mol. Biol.* **117**, 1-31.

Kirschner, M. and Mitchison, T. (1986). Beyond self-assembly: from microtubules to morphogenesis. *Cell* **45**, 329-342.

Kline-Smith, S. L. and Walczak, C. E. (2004). Mitotic spindle assembly and chromosome segregation: refocusing on microtubule dynamics. *Mol. Cell* **15**, 317-327.

Komarova, Y. A., Akhmanova, A. S., Kojima, S., Galjart, N. and Borisy, G. G. (2002a). Cytoplasmic linker proteins promote microtubule rescue in vivo. *J. Cell Biol.* **159**, 589-599.

Komarova, Y. A., Vorobjev, I. A. and Borisy, G. G. (2002b). Life cycle of MTs: persistent growth in the cell interior, asymmetric transition frequencies and effects of the cell boundary. *J. Cell Sci.* **115**, 3527-3539.

Maly, I. V. (2002). Diffusion approximation of the stochastic process of microtubule assembly. *Bull. Math. Biol.* **64**, 213-238.

McNally, F. (2003). Microtubule dynamics: new surprises from an old MAP. *Curr. Biol.* **13**, R597-R599.

Mitchison, T. and Kirschner, M. (1984). Dynamic instability of microtubule growth. *Nature* **312**, 237-242.

Mitchison, T. J. and Kirschner, M. W. (1987). Some thoughts on the partitioning of tubulin between monomer and polymer under conditions of dynamic instability. *Cell Biophys.* **11**, 35-55.

Musch, A. (2004). Microtubule organization and function in epithelial cells. *Traffic* **5**, 1-9.

Odde, D. J. (1997). Estimation of the diffusion-limited rate of microtubule assembly. *Biophys. J.* **73**, 88-96.

Oosawa, F. and Asakura, S. (1975). *Thermodynamics of the Polymerisation of Protein*. New York: Academic Press.

Oosawa, F. and Kasai, M. (1962). A theory of linear and helical aggregations of macromolecules. *J. Mol. Biol.* **4**, 10-21.

Piehl, M., Tulu, U. S., Wadsworth, P. and Cassimeris, L. (2004). Centrosome maturation: measurement of microtubule nucleation throughout the cell cycle by using GFP-tagged EB1. *Proc. Natl. Acad. Sci. USA* **101**, 1584-1588.

Rogers, S. L. and Gelfand, V. I. (2000). Membrane trafficking, organelle transport, and the cytoskeleton. *Curr. Opin. Cell Biol.* **12**, 57-62.

Rusan, N. M., Fagerstrom, C. J., Yvon, A. M. and Wadsworth, P. (2001). Cell cycle-dependent changes in microtubule dynamics in living cells expressing green fluorescent protein-alpha tubulin. *Mol. Biol. Cell* **12**, 971-980.

VanBuren, V., Odde, D. J. and Cassimeris, L. (2002). Estimates of lateral and longitudinal bond energies within the microtubule lattice. *Proc. Natl. Acad. Sci. USA* **99**, 6035-6040.

Verde, F., Dogterom, M., Stelzer, E., Karsenti, E. and Leibler, S. (1992). Control of microtubule dynamics and length by cyclin A- and cyclin B-dependent kinases in Xenopus egg extracts. *J. Cell Biol.* **118**, 1097-1108.

Wang, H. W. and Nogales, E. (2005). Nucleotide-dependent bending flexibility of tubulin regulates microtubule assembly. *Nature* **435**, 911-915.

Wollman, R., Cytrynbaum, E. N., Jones, J. T., Meyer, T., Scholey, J. M. and Mogilner, A. (2005). Efficient chromosome capture requires a bias in the 'search-and-capture' process during mitotic-spindle assembly. *Curr. Biol.* **15**, 828-832.

Zimmerman, S. and Chang, F. (2005). Effects of {gamma}-tubulin complex proteins on microtubule nucleation and catastrophe in fission yeast. *Mol. Biol. Cell* **16**, 2719-2733.